NRL Memorandum Report 4671

# Weak and Strong Ignition
# II. Sensitivity of the Hydrogen-Oxygen System

E. S. ORAN AND J. P. BORIS

*Laboratory for Computational Physics*



December 7, 1981

This research was sponsored by the Office of Naval Research and the Naval Material Command.



NAVAL RESEARCH LABORATORY
Washington, D.C.

SECURITY CLASSIFICATION OF THIS PAGE (When Data Entered)

| REPORT DOCUMENTATION PAGE | | READ INSTRUCTIONS BEFORE COMPLETING FORM |
|---|---|---|
| 1. REPORT NUMBER<br>NRL Memorandum Report 4671 | 2. GOVT ACCESSION NO.<br>AD-A108 | 3. RECIPIENT'S CATALOG NUMBER<br>843 |
| 4. TITLE (and Subtitle)<br>WEAK AND STRONG IGNITION<br>II. SENSITIVITY OF THE HYDROGEN-OXYGEN SYSTEM | | 5. TYPE OF REPORT & PERIOD COVERED<br>Interim report on a continuing NRL problem.<br>6. PERFORMING ORG. REPORT NUMBER |
| 7. AUTHOR(s)<br>E.S. Oran and J.P. Boris | | 8. CONTRACT OR GRANT NUMBER(s) |
| 9. PERFORMING ORGANIZATION NAME AND ADDRESS<br>Naval Research Laboratory<br>Washington, DC 20375 | | 10. PROGRAM ELEMENT, PROJECT, TASK AREA & WORK UNIT NUMBERS<br>RR0130144 & ZF43451001;<br>44-0572-01 & 44-0061-A1 |
| 11. CONTROLLING OFFICE NAME AND ADDRESS<br>Office of Naval Research<br>Washington, DC 22217 | | 12. REPORT DATE<br>December 7, 1981<br>13. NUMBER OF PAGES<br>39 |
| 14. MONITORING AGENCY NAME & ADDRESS(if different from Controlling Office) | | 15. SECURITY CLASS. (of this report)<br>UNCLASSIFIED<br>15a. DECLASSIFICATION/DOWNGRADING SCHEDULE |

16. DISTRIBUTION STATEMENT (of this Report)

Approved for public release; distribution unlimited.

17. DISTRIBUTION STATEMENT (of the abstract entered in Block 20, if different from Report)

18. SUPPLEMENTARY NOTES

This research was sponsored by the Office of Naval Research and the Naval Material Command.

19. KEY WORDS (Continue on reverse side if necessary and identify by block number)

Combustion
Shock tubes
Detonations
Hydrogen-oxygen combustion

20. ABSTRACT (Continue on reverse side if necessary and identify by block number)

This paper identifies the physical and chemical mechanisms which cause certain mixtures of hydrogen, oxygen and argon to be very sensitive to sound wave or entropy (temperature) perturbations. Detailed simulations of the effects of sound waves in typical mixtures are used to show explicitly the effects of such fluctuations on the chemical induction time. A quantity, $\Delta\tau_{max}$, is defined which represents the maximum variation produced in the chemical induction time of a system given the amplitude and frequency

(Continues)

DD FORM 1 JAN 73 1473 EDITION OF 1 NOV 65 IS OBSOLETE
S/N 0102-014-6601

SECURITY CLASSIFICATION OF THIS PAGE (When Data Entered)

20. ABSTRACT (Continued)

of a perturbation. It is observed that these perturbations may cause ignition to occur unevenly in such mixtures and this leads to ignition which appears spotty. Using detailed numerical simulations and a generalized induction parameter model derived from it, $\Delta\tau_{max}$ is evaluated and a criterion is developed for spotty and smooth ignition behind reflected shock waves. These effects are related to weak and strong ignition observed in shock tube experiments.

CONTENTS

# WEAK AND STRONG IGNITION
# II. SENSITIVITY OF THE HYDROGEN-OXYGEN SYSTEM

## I. Introduction

In a previous paper [1], refered to below as Paper I, we compared data from experiments on reflected shocks in hydrogen-oxygen-argon mixtures [2] to corresponding detailed numerical simulations. We found that simulations of the conditions behind the reflected shock in what is called the strong ignition regime of the pressure-temperature plane gave results which are in close quantitative agreement to those observed experimentally. A fairly sharp, uniform reaction wave starts at the reflecting wall after the chemical induction time has elapsed. Simulations for physical and chemical conditions which fall in the weak ignition regime also displayed behavior analogous to experiments. Here the reaction wave starts at some time earlier than the chemical induction time at a location away from the reflecting wall. Analyses of the results indicate that simulations of both the strong and weak cases had very similar numerical perturbations. However, the weak ignition system was much more sensitive to nonuniformities existing behind the reflected shock.

The differences in behavior called "strong" (or "sharp") ignition, and "weak" (or "mild") ignition, were first noted by Soloukhin and Strehlow and their coworkers [3,4,5,6,7,8] (See primarily Strehlow and Cohen [3] and Voevodsky and Soloukhin [8]). The later work of Meyer and Oppenheim [9] showed that the reaction wave started at some location away from the reflecting wall in the weak ignition case. Both Voevodsky and Soloukhin and Meyer and Oppenheim used their experiments to try to delineate a universal dividing line on the pressure-temperature plane. Meyer and Oppenheim [9] and Borisov [10] pointed out the sensitivity of certain systems to fluctuations.

Manuscript submitted September 28, 1981.

In this paper we identify and isolate those mechanisms which we believe cause the sensitivity of certain systems to sound wave and entropy perturbations. First we show that chemical sensitivity can be represented in terms of derivatives of the chemical induction time with respect to temperature at constant entropy and at constant pressure. We then study in detail the effects of sound wave perturbations on both a weak and a strong ignition case. This study reveals that in the weak ignition case, the time-rate-of-change of the radicals H, O, and OH show an increase in time which is faster than exponential for a long period of time prior to ignition. This is contrasted to the classical exponential behavior exhibited by the strong ignition case. We then use this information to derive a simplified but quantitative induction time model which gives criteria for the maximum variations produced in induction times in a system, $\Delta\tau_{max}$, given the amplitude and frequency of sound wave perturbations.

We also observe that the presence of a perturbation may cause ignition to occur first at some location which is heated at a later time by the shock than other locations. This causes what appears to be spotty ignition. We show that the conditions which allow ignition to be spotty depend only on the state of the system before any energy is released. A communication effect due to the propagation of pressure pulses once energy has been released would tend to decrease $\Delta\tau_{max}$. We then combine the calculations of $\Delta\tau_{max}$ and the criterion for spotty ignition to explain the experimentally observed weak and strong ignition phenomena.

On a slightly different but related track, Toong and coworkers have done extensive work showing the effect of nonequilibrium chemical kinetics on the propagation of sound waves [11,12,13,14,15] Toong [11] has shown theoretically that acoustic waves may e amplified or attenuated due to changes in mean conditions resulting from chemical reactions and due to fluctuations in reaction rates due to acoustic waves. In this paper we emphasize the effects of sound wave perturbations on chemical kinetics and show how these perturbations may cause confusion in the interpretation of experiments.

## II. Sensitivity of the Chemical Induction Time

Previous work on an induction parameter model [16] has required that we evaluate the chemical induction time, $\tau_i$, for the ratio $H_2$:$O_2$:X/2:1:4 where X is diluent. The curves on Figure 1, which show $\tau_i$ (2:1:4) for a wide range of pressures and temperatures, were calculated by integrating the ordinary differential equations describing the chemical rate scheme given in Paper I. This scheme has been extensively tested against experiments and shown to predict induction times accurately [17]. We note that in this paper the induction time is defined as that time at which there is a noticeable ($\sim 20^{\circ}K$) rise in initial temperature.

Subsequently we have found that the induction times for many other dilutions and stoichiometries (where the amounts of $H_2$:$O_2$:Ar are in the ratios of a:b:X)may be obtained to excellent approximation from the formula

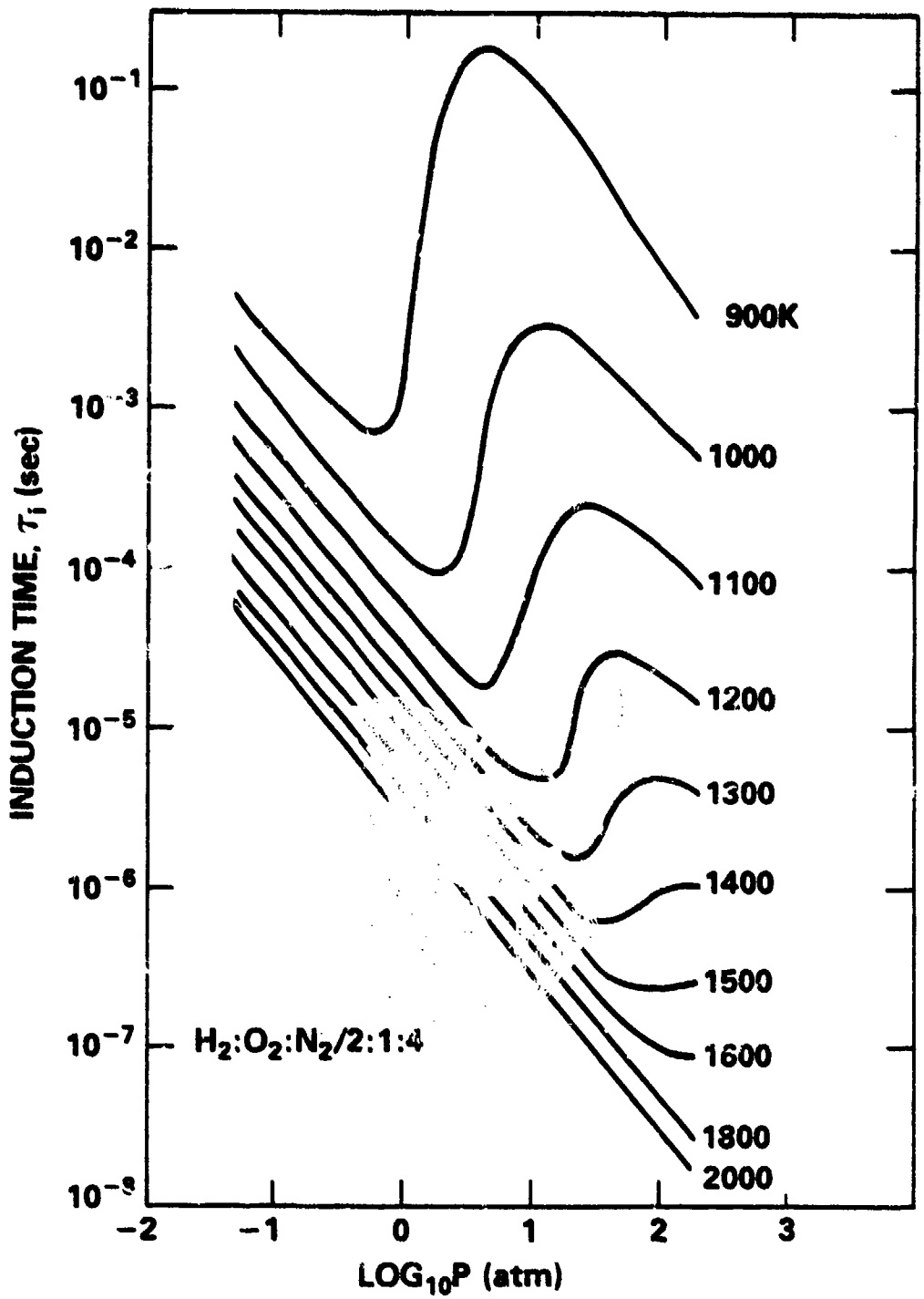


Fig. 1 — Chemical induction time as a function of pressure at selected temperatures for homogeneous mixtures of $H_2$:$O_2$:Ar/2:1:4 derived from the detailed rate scheme given in Paper I [1]

$$\tau_i\ (a,b,X) = R(a,b,X)\ \tau_i(2:1:4) \tag{1}$$

where

$$R(a,b,X) = \frac{1}{2}\left[\frac{2(a+b+X)}{7a} + \frac{a+b+X}{7b}\right] \quad . \tag{2}$$

Tests of the predictions of Equations (1) and (2) against detailed integration of the chemical rate equations indicate that this model works well for the three cases in which we will be interested here, 2:1:0, 2:1:7 and 8:2:90. The first case, 2:1:0, is the case for which Voevodsky and Soloukhin [8], and Meyer and Oppenheim [9] did their shock tube studies of weak and strong ignition. The second two cases, 2:1:7 and 8:2:90, are those used in the shock tube experiments and detailed numerical simulations in Paper I. Figures 2a, b and c show contours of $\tau_i$ on the pressure temperature plane in the range $0.5 \leq P \leq 6$ atm and $900 \leq T \leq 1100^{\circ}K$. Taken together these show the expected effect of diluting the reactive gases.

The data in Figure 2 were then used to evaluate the quantities

$$\frac{-T}{\tau_i}\ \frac{\partial \tau_i}{\partial T}\bigg|_P \quad \text{and} \quad \frac{-T}{\tau_i}\ \frac{\partial \tau_i}{\partial T}\bigg|_S \tag{3a}$$

which reflect the sensitivity of $\tau_i$ to entropy (temperature) variations at constant pressure P and sound waves at constant entropy S. The constant pressure derivative was found directly from the data. However, the constant entropy derivative is a combination of two terms:

$$\frac{T}{\tau_i}\ \frac{\partial \tau_i}{\partial T}\bigg|_S = \frac{\gamma}{\gamma-1}\ \frac{P}{T}\ \frac{\partial \tau_i}{\partial P}\bigg|_T + \frac{\partial \tau_i}{\partial T}\bigg|_P . \tag{3b}$$

where $\gamma$ is the ratio of specific heats, $C_p/C_v$. The second term on the right hand side of Equation (3) is always negative. Although the first term, as seen in Figure (1), may be either positive or negative, the weighted sum is always negative. Figure (3) shows the constant entropy derivative

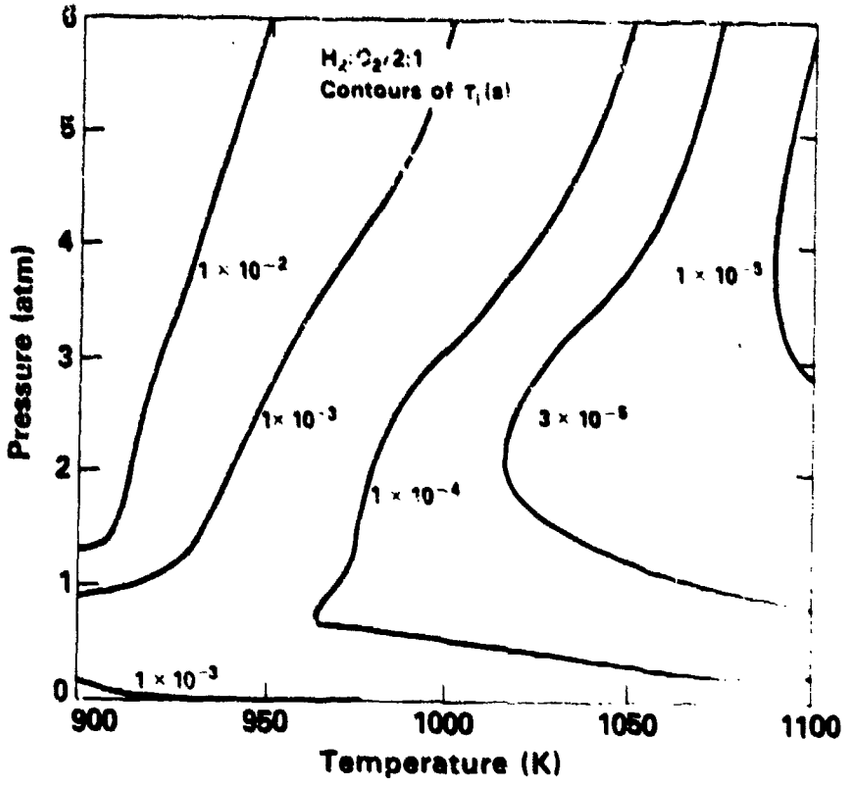


Fig. 2a — Contours of constant chemical induction time (in seconds) as a function of temperature and pressure for the mixture $H_2$:$O_2$/2:1

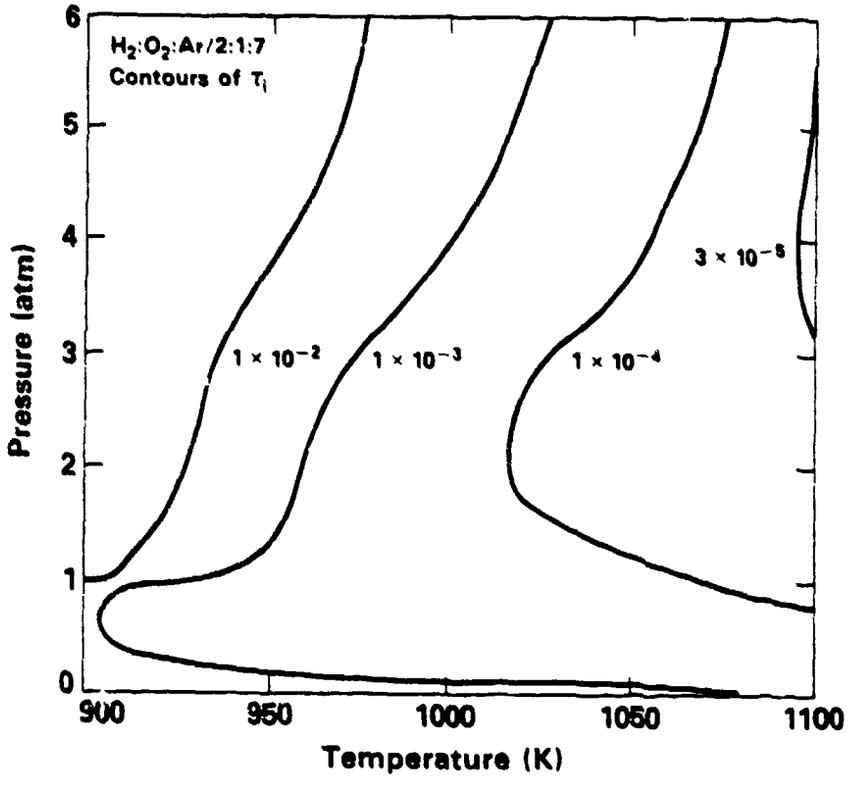


Fig. 2b — Same as Fig. 2a for $H_2$:$O_2$:Ar/2:1:7

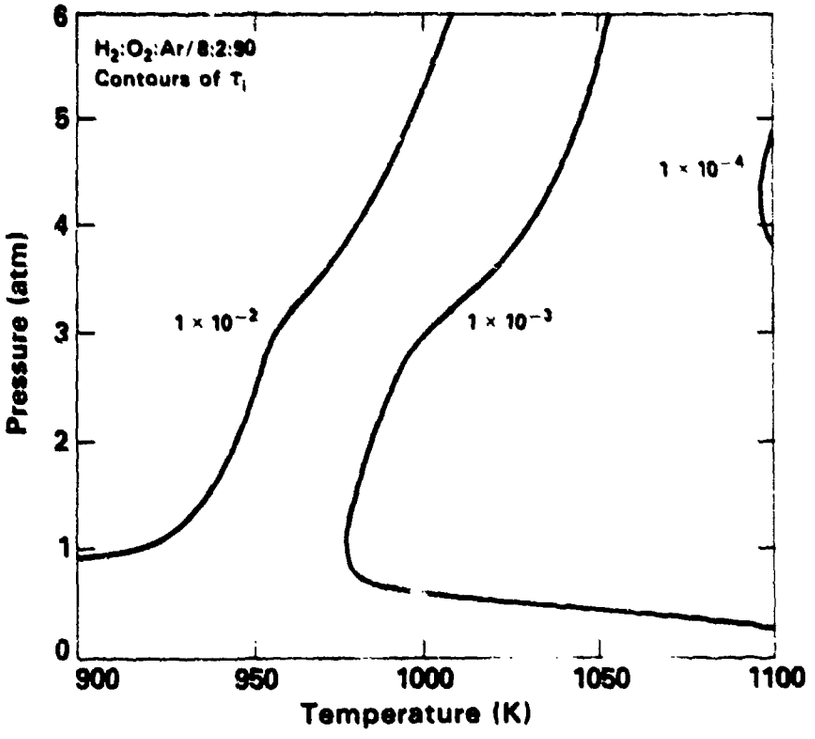


Fig. 2c — Same as Fig. 2a for $H_2$:$O_2$:Ar/8:2:90

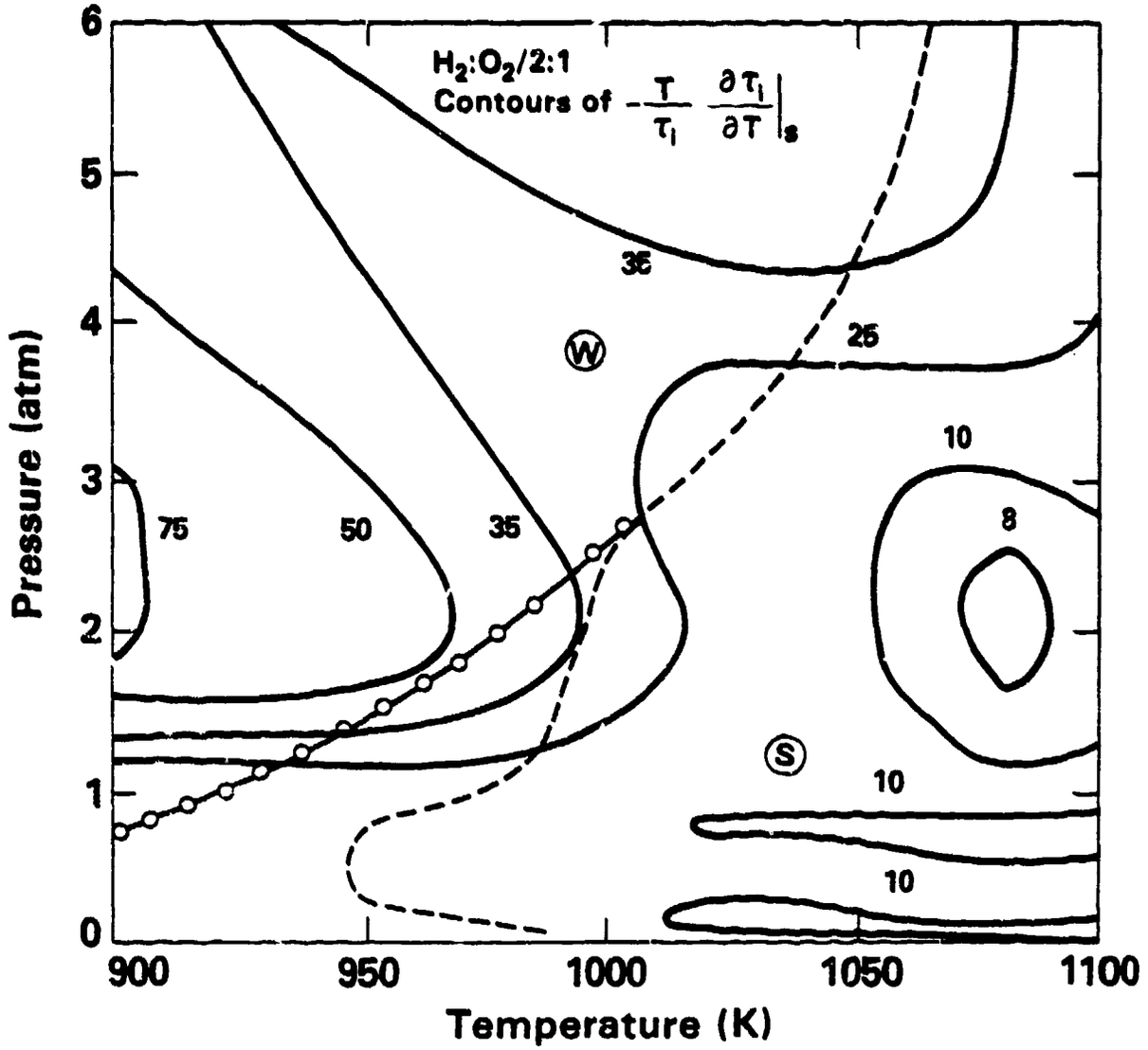


Fig. 3 — The solid lines are contours of the sensitivity parameter to perturbations at constant entropy (sound waves). The line of open circles indicates the extended second limit. The dashed line indicates the division between weak and strong ignition derived by Meyer and Oppenheim [9].

for the 2:1:0 case and Figure 4 shows the constant pressure derivative. We note that high values of the derivative indicate that the system is more sensitive for those values of pressure and temperature.

The results for the 2:1:7 and 8:2:90 cases are not shown because they are virtually identical to those for 2:1:0. Equations (1) and (2) in fact predict the independence of the sensitivity derivatives (3a) and (3b) to variations in stoichiometry and dilution and hence predicts their universality. This report has been tested against detailed calculations in a number of regimes and agreement is excellent. However, the universality can only be derived under the assumption that binary reactions dominate the determination of the induction time.

Superimposed on these contours are the criteria for separating weak and strong ignition given by Voevodsky and Soloukhin [8] and Meyer and Oppenheim [9]. Voevodsky and Soloukhin suggested that the criterion is related to the extended second limit, which is defined by the competition between chain branching and termolecular recombination of H and $O_2$. Thus a line is defined on the pressure-temperature plane at $2k_2 = k_3$, where $k_2$ and $k_3$ are the chemical reaction rates for $H + O_2 \rightarrow OH + O$ and $H + O_2 + M \rightarrow HO_2 + M$, respectively. The criterion suggested by Meyer and Oppenheim is based on their experiments. We note that both criteria separate more sensitive from less sensitive regions, although it is not obvious how to derive these results from the chemical sensitivities shown.

## III. Detailed Simulations of Sound Wave Perturbations

In order to evaluate how the sensitivities discussed above effect ignition, we have performed a number of detailed simulations of a sound

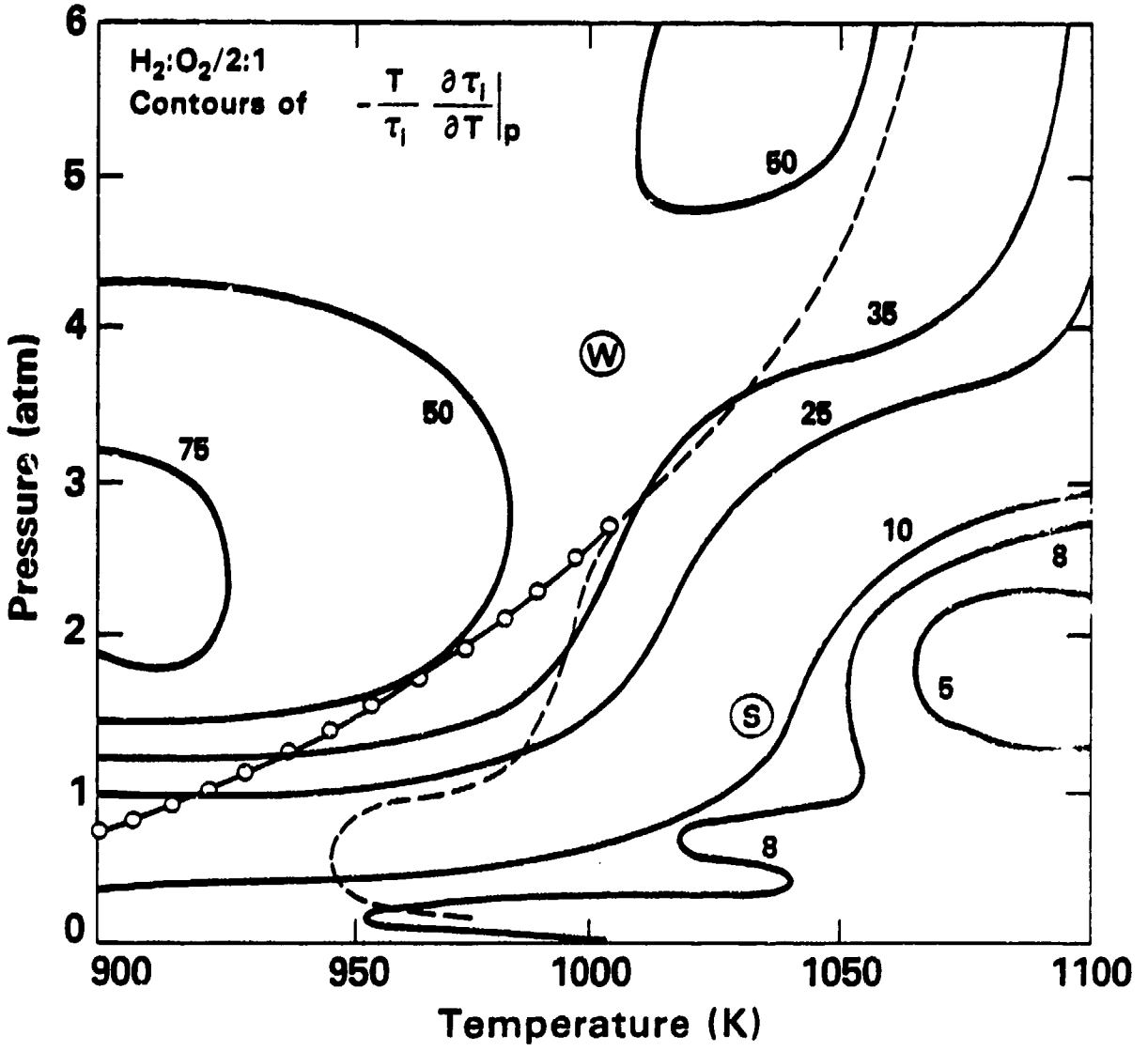


Fig. 4 — Same as Fig. 3 except contours are for perturbation at constant pressure

wave in a reactive mixture. These used the one-dimensional, time-dependent NRL reactive shock model described extensively in Paper I and references [18] and [16]. This model combines the Flux-Corrected Transport algorithm for convective transport [19,20] with the CHEMEQ algorithm to solve the ordinary differential equation describing the chemical kinetics [21,22]. Coupling these processes has been described by Oran and Boris [23]. The chemical rate scheme used is the same one which generated the induction times shown in Figure 1 [1].

Consider a uniform region with homogeneous mixtures of hydrogen, oxygen, and argon at the temperatures and pressures shown in Table I. These are the two cases for which detailed shock tube simulations were described in Paper I. Then at the beginning of the calculation the velocity perturbation shown in Figure 5 is imposed on the system at each location x such that

$$v(x,t=0) = v_o \sin(\frac{\pi}{S_L} x) \qquad (4)$$

where $v_o$ is the amplitude and $S_L$ is the half wavelength of the sound wave perturbation. We determine S by deciding how many periods of the wave we wish to occur during a chemical induction time.

Figure 6 and 7 show the results of simulation of the two cases in Table I. For these calculations there were roughly three periods of sound wave oscillation in an induction time. This means that $S_L$ is 1.17 cm for the strong ignition case and 15 cm for the weak case. A relatively large amplitude perturbation, $v_o = 1 \times 10^4$ cm/sec, was chosen. For the strong ignition case, shown in Figure 6, the system ignites first at the right hand wall at about 85 μs, then at the center and left hand wall and at 92 μs. Thus we observed that $\Delta\tau_{max}$, which measures the time difference for ignition throughout the system,

Table I

| | Weak Ignition | Strong Ignition |
|---|---|---|
| Temperature | 1000 K | 1034 K |
| Pressure | 3.72 atm | 1.3 atm |
| Induction Time | 1550 μs | 109 μs |
| Stoichiometry | 8:2:90 | 2:1:7 |

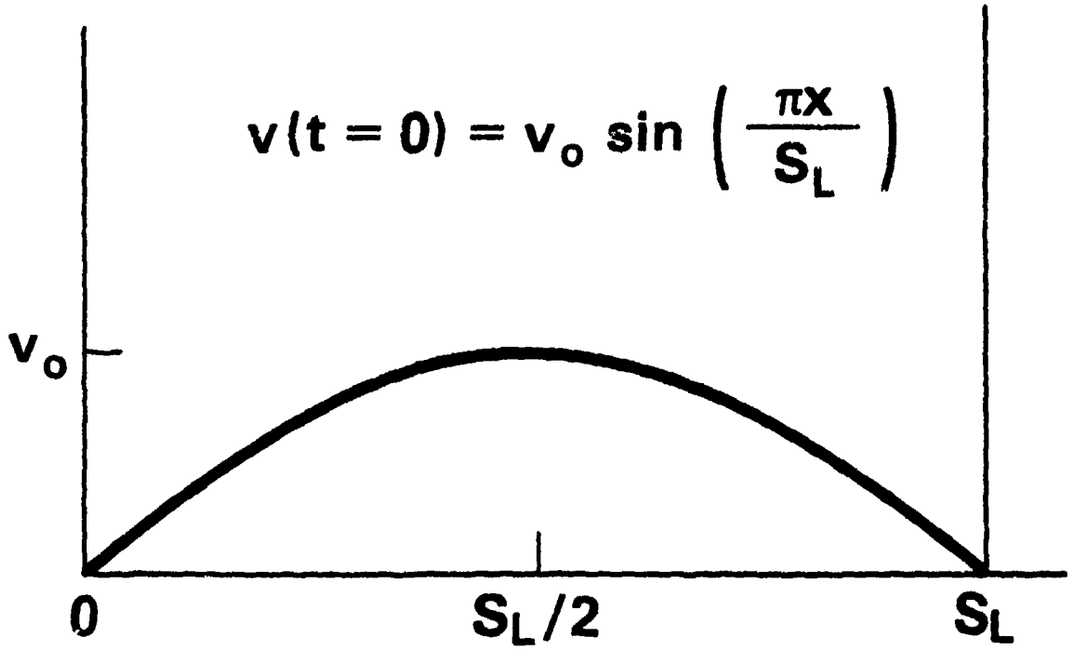


Fig. 5 — Velocity perturbation used to initialize the simulation to test the influence of sound waves on ignition

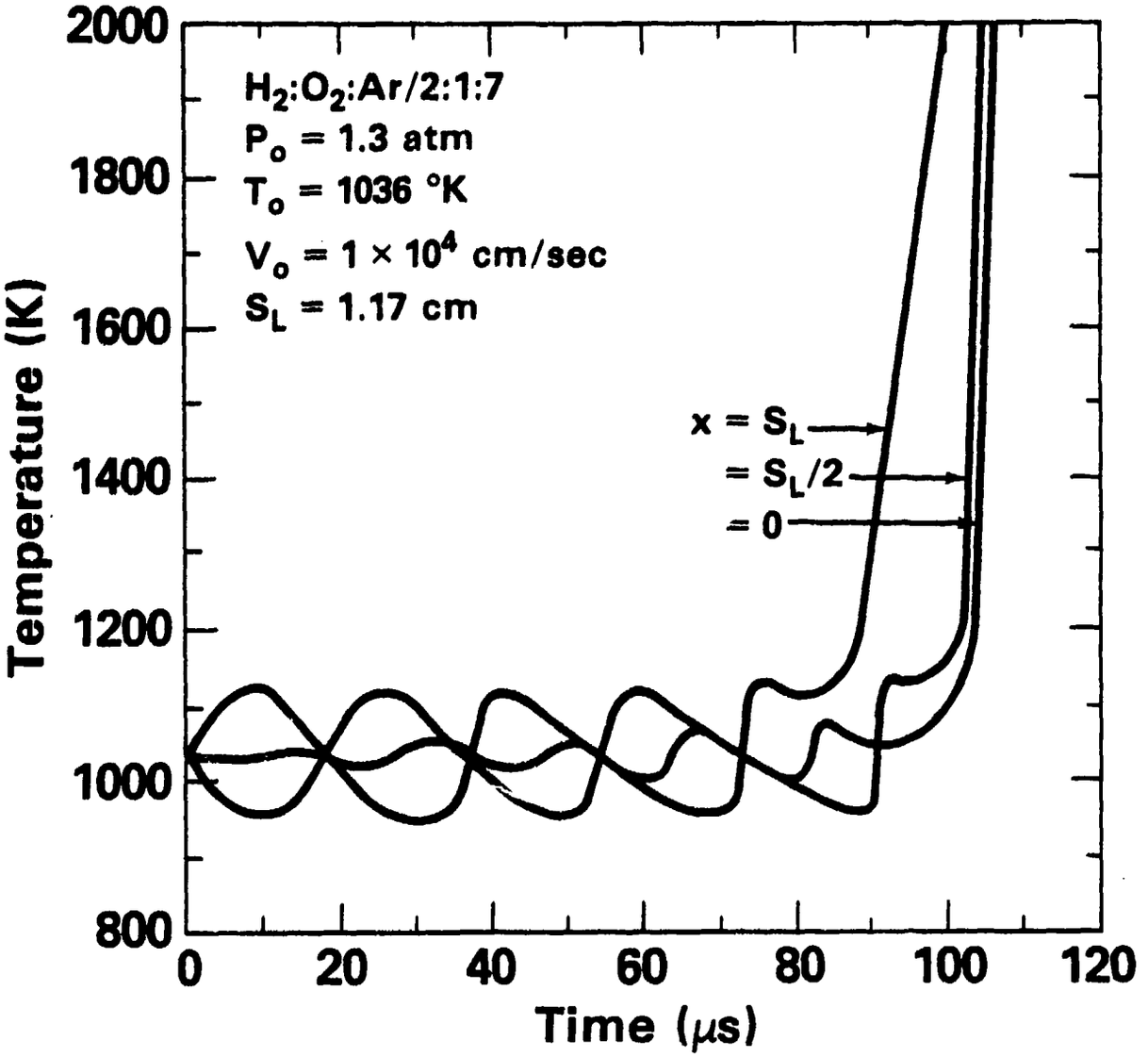


Fig. 6 — Temperature as a function of time for three locations in the sound wave simulation in the strong ignition regime

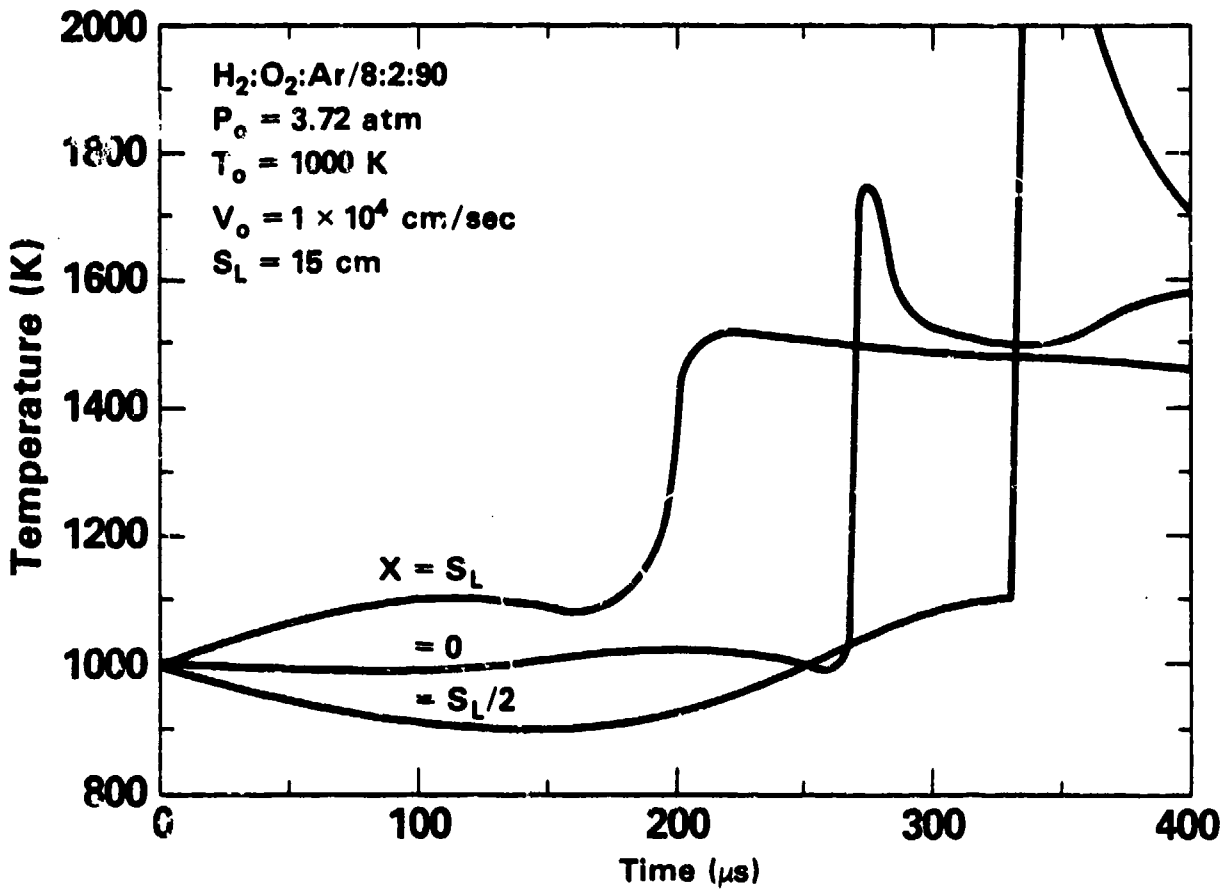


Fig. 7 — Same as Fig. 6 but a weak ignition case

is 7 μsec in this case. This is a very small delay which would barely be observable in the schlieren photographs, even at this relatively large fluctuation amplitude. Note that without the sound wave perturbation the system ignites at 109 μs. Figure 7 is an analogous graph for the weak ignition case. Here we observe that the right hand wall ignites at about 160 μs, an order of magnitude earlier in time than the unperturbed case. The ignition then generates a detonation wave which propagates back through the system (Figure 8). Figure 9 shows the results of perturbing the weak ignition system by a much smaller amplitude, $v_o = 5 \times 10^2$ cm/sec. Here we observe that $\Delta\tau_{max} = 50$ μsec and the system first ignites about 75 μs earlier than if there had been no perturbation.

These simulations show us that there are two effects occurring which cause various locations in the system to have different induction times. The first effect is caused by compression and the resulting temperature change due to the presence of the sound wave. The second effect is a communication effect which only occurs after energy has been released. The first effect is clearly present in Figures 6, 7 and 9. The second effect is only obvious in Figure 7, as seen in the propagating detonation wave in Figure 8. However, energy release itself generates sound waves which propagate away from the ignition center. Thus the influence of one location igniting may be felt by its neighbors.

Much of what has been said about the influence of sound waves on ignition also applies to entropy waves. These types of fluctuations generate sound waves which are the major mode of communication in systems

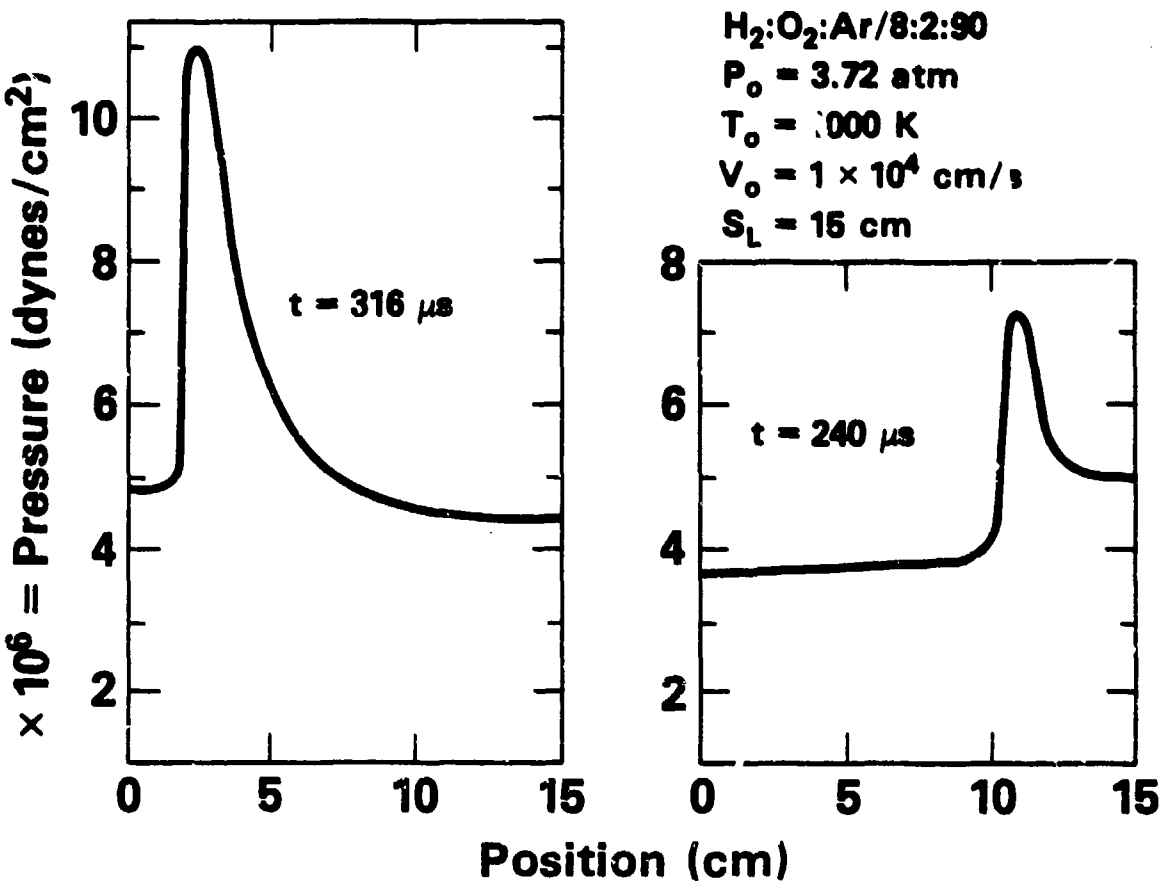


Fig. 8 — Calculated pressure as a function of position at two times after ignition in the weak ignition case

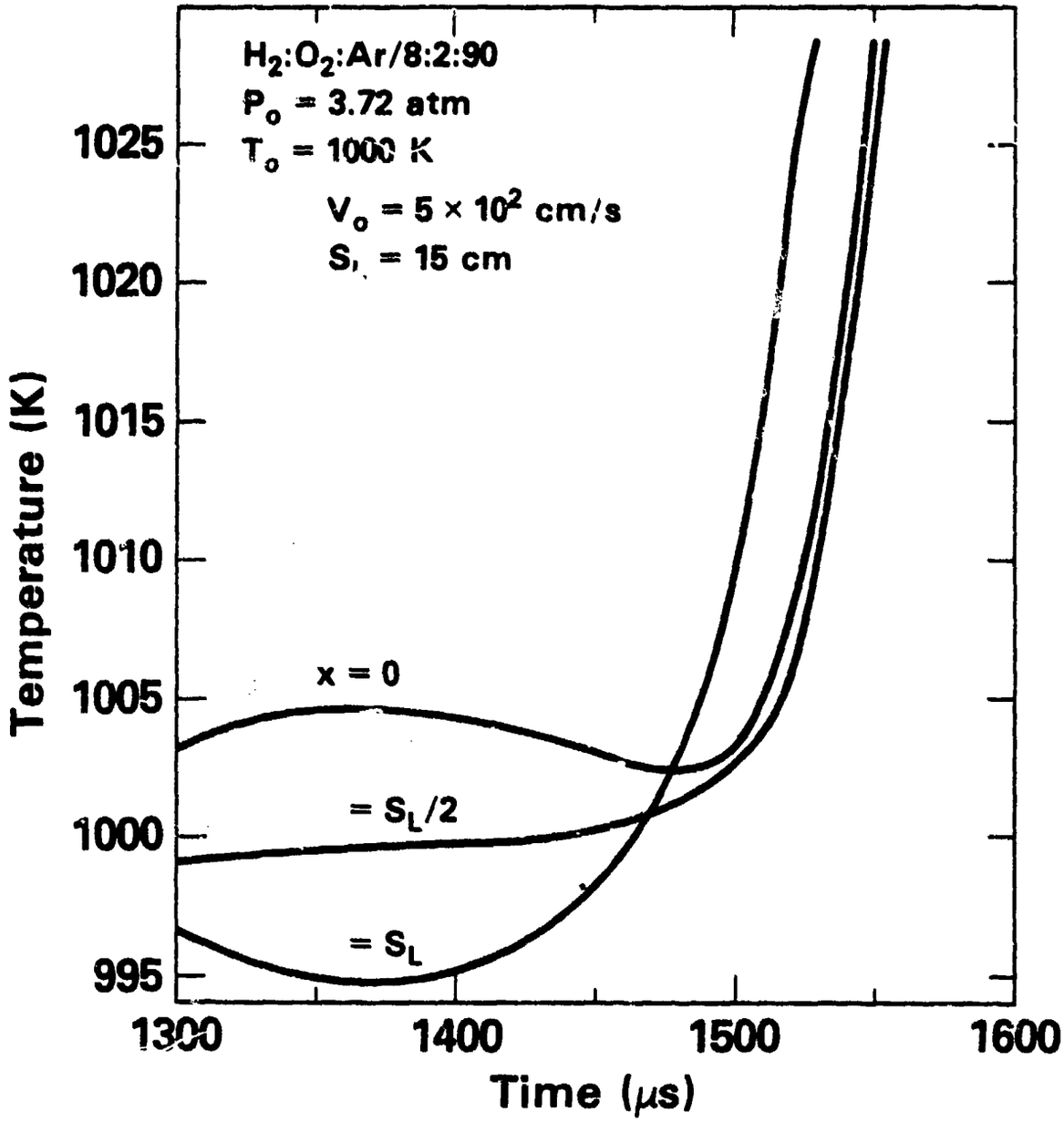


Fig. 9 — Same as Fig. 7 but with a weaker perturbation

where thermal conduction is of negligible importance. As seen in Figure 4 as well as Figure 3, there is a large difference in sensitivity between the weak and strong ignition cases.

## IV. "Spotty" and "Smooth" Ignition

The contours shown in Figures 2, 3, and 4, the detailed sound wave simulations shown in Figures 6, 7, 8, and 9 and the detailed shock tube simulations in Paper I are convincing evidence that certain systems are very sensitive to entropy mode and sound wave perturbations. We proceed now to explore how these sensitivities are related to the mechanisms causing weak and strong ignition.

Consider first Figures 10a and b. The slope of the straight lines in both figures represent velocities at which the reflected shock moves away from the reflecting wall and thus the rate of change of position at which material is first subjected to the higher temperature and pressure. Each fluid element has associated with it a time, $\tau_i$, at which it begins to release energy. The wavy lines superimposed on the straight line represent the effects of perturbations in the gas which locally alter the induction time from $\tau_i$. Thus we see in Figure 10b that for large enough velocities of the reflected shock, and large enough amplitude fluctuations or small enough wavelength fluctuations, ignition can first occur at some location away from the wall. It might, in fact, occur at several places essentially simulataneously. This is the effect observed in the weak ignition calculations and experiments described above. We shall call the situation illustrated in Figure 10a "smooth" ignition, because ignition propagates smoothly from the reflecting wall even though the rate may show a small fluctuation about the mean.

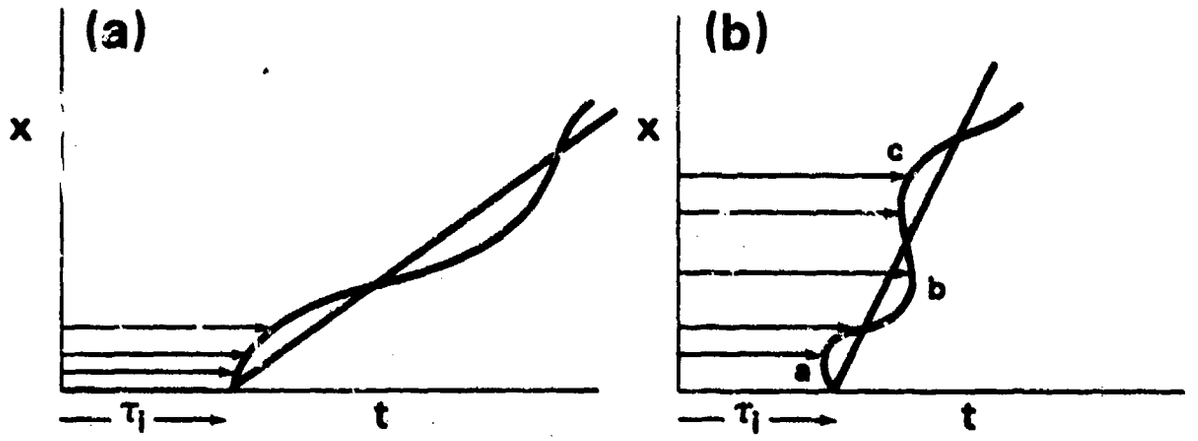


Fig. 10 — Schematic illustration indicating how ignition in a system with small fluctuations may be smooth (10a) or spotty (10b)

We shall call the situation illustrated in Figure 10b "spotty" ignition, because ignition can occur in what appears to be a discontinuous or spotty fashion.

Finally we note that there is a communication effect between fluid elements which depends on the speed of sound in the mixture. This will tend to diminish but not totally destroy spotty ignition as pressure and temperature increases due to energy release are communicated. For example, from Figure 6 we see that $\Delta\tau_{max}$ = 15 μs and since the sound speed is $\sim 6\times10^4$ cm/s, the material at the two end walls ignites independently. Similar arguments about communication hold for the calculations shown in Figure 9, where $\Delta\tau_{max} = \sim 40$ μs. However, it is very clear in Figure 7 where $\Delta\tau_{max}$ = 150 μs that it is the ignition at $x=S_L$ that induces early ignition at x = C. This is due to the generation of a detonation wave which propagates back into the mixture and ignites it. Thus we see that the idealized sound wave calculations presented above had intermingled both the smooth-spotty and the communication effects.

For the case of a sound perturbation shown in Figure 10 wave we may write

$$\tau_i(x) = \frac{x}{v_R} + \frac{\Delta\tau_{max}}{2} \sin \frac{\pi x}{S_L} \tag{5}$$

where $\tau_i$ (x) is the induction time at some location x, $v_R$ is the velocity of the reflected shock, $\Delta\tau_{max}$ is the maximum deviation in $\tau_i$ due to fluctuations and $2S_L$ is the wavelength of the perturbation. By writing

$$\frac{\partial\tau_i}{\partial x} - 0 = \frac{1}{v_R} + \frac{\pi}{S_L} \frac{\Delta\tau_{max}}{2} \cos \frac{\pi x}{S_L} \tag{6}$$

we determine that the condition for spotty ignition is

$$\Delta\tau_{max} > \frac{S_L}{\pi} \frac{2}{v_R} \quad . \tag{7}$$

The quantity $\Delta\tau_{max}$ is a time which depends on the strength and frequency of the fluctuation. The quantity $v_R$ is a property of the incident shock. Then from the sound speed in the material and $S_L$, we can assess whether or not communication effects may be important.

## V. Evaluation of $\Delta\tau_{max}$

In order to study the weak-strong ignition phenomena in shock tubes, we performed the detailed simulations of reflecting shocks shown in Paper I. Then to isolate the phenomena we thought were causing the weak ignition, we investigated the interactions of chemical reactions and sound waves. Now we carry this simplification one step further by attempting to further quantify the mechanism which leads to the condition of Equation (7) and is responsible for spotty and smooth ignition due to sound wave perturbations. This requires calculating $\Delta\tau_{max}$ in terms of amplitude, frequency, and properties of the shocked fluid.

Figure 11 shows plots of the logorithm of d[OH]/dt as a function of the logorithm of [OH] for both the weak and strong ignition cases listed in Table I. Also shown are times at which specific densities of [OH] are reached. Since these curves have been derived by integrating only the ordinary differential equations describing the chemical kinetics scheme given in Paper I, no fluid dynamic effects are present. Throughout the time period for which these curves are plotted, there has been no significant energy release in the system. First note that the values of [OH] shown for the weak ignition case are between $10^{10}$ and $10^{13}$ $cm^{-3}$ where the total number densities are about $10^{19}$ $cm^{-3}$. The slope from relatively early in the calculation to the point of ignition is very close to 4/3. The behavior below $10^{10}$ $cm^{-3}$ is less easily defined by a single exponent. In fact there appears to be a very fast rise, perhaps a linear phase, until it joins the line of slope 4/3 at $10^{10}$ $cm^{-3}$. Systems which have the same entropy (i.e., different phases of the same sound wave) show the same qualitative behavior, although they differ in ignition time and at the specific density at which the slope becomes 4/3. For example, in the case

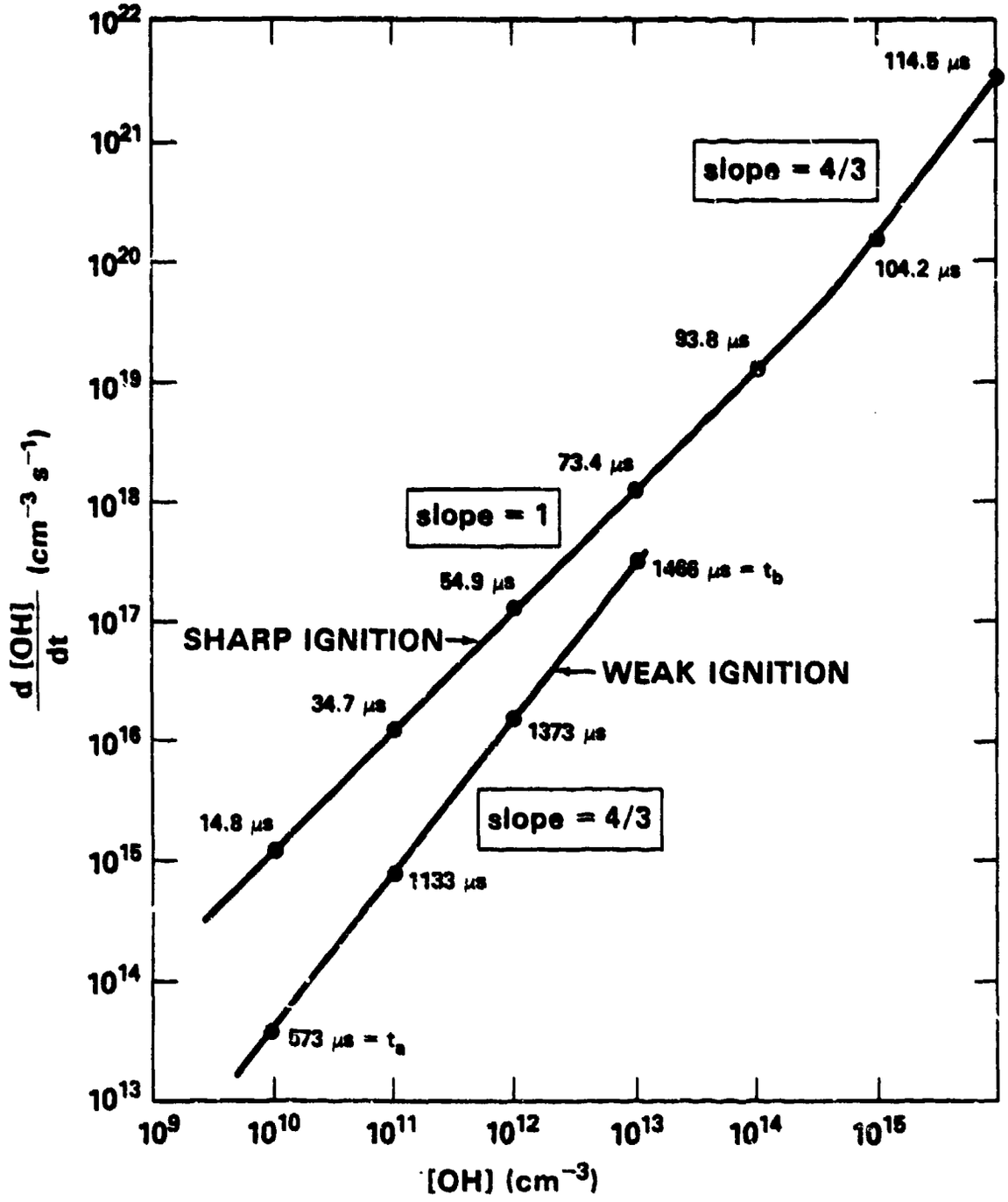


Fig. 11 — Calculated time-rate-of-change and OH density as a function of OH density for the weak and strong ignition cases studied

when T = 1020 K and P = 3.92 atm, which has the same entropy as the weak ignition case in Table I, the slope becomes 4/3 when $[OH]=3\times10^{10}$ $cm^{-3}$ and $\tau_i$ = 666 μs. Figure 12 shows that [H] and [O] and to some extent $[HO_2]$ are locked into this 4/3 behavior also.

Now consider the strong ignition line on Figure 11. Here the slope is almost always 1, although it appears to transition to the 4/3 behavior just prior to ignition. Again we note that isentropes of these conditions show the same qualitative behavior. The slope 1 behavior has been previously described by, for example, Schott and Getzinger [24] and has been used by Brokaw [25] to describe the hydrogen-oxygen reaction scheme.

In real time, the slope 1 region is much earlier than the slope 4/3 region. In fact, we know from studying the computations in detail that the slope 1 region is associated with domination of the mechanism by chain branching reactions such as $O + H_2 \rightarrow OH + H$ or $H + O_2 \rightarrow OH + O$, and the slope 4/3 region seems to be associated with the termolecular buildup of $HO_2$, through the reaction $H + O_2 + M \rightarrow HO_2 + M$.

Having observed the behavior of the slope of [OH] for the weak ignition case and its isentropes, we exploit this very well defined behavior to develop a simplified theory to evaluate the $\Delta\tau_{max}$ required in Equation (7). From Figures 13a and 13b, which expand the early time behavior of OH in Figure 11, we know that we can write

$$\frac{dn}{dt} = \frac{S_{-1}}{n} + S_o + S_1 n + S_{4/3} n^{4/3} \qquad (8)$$

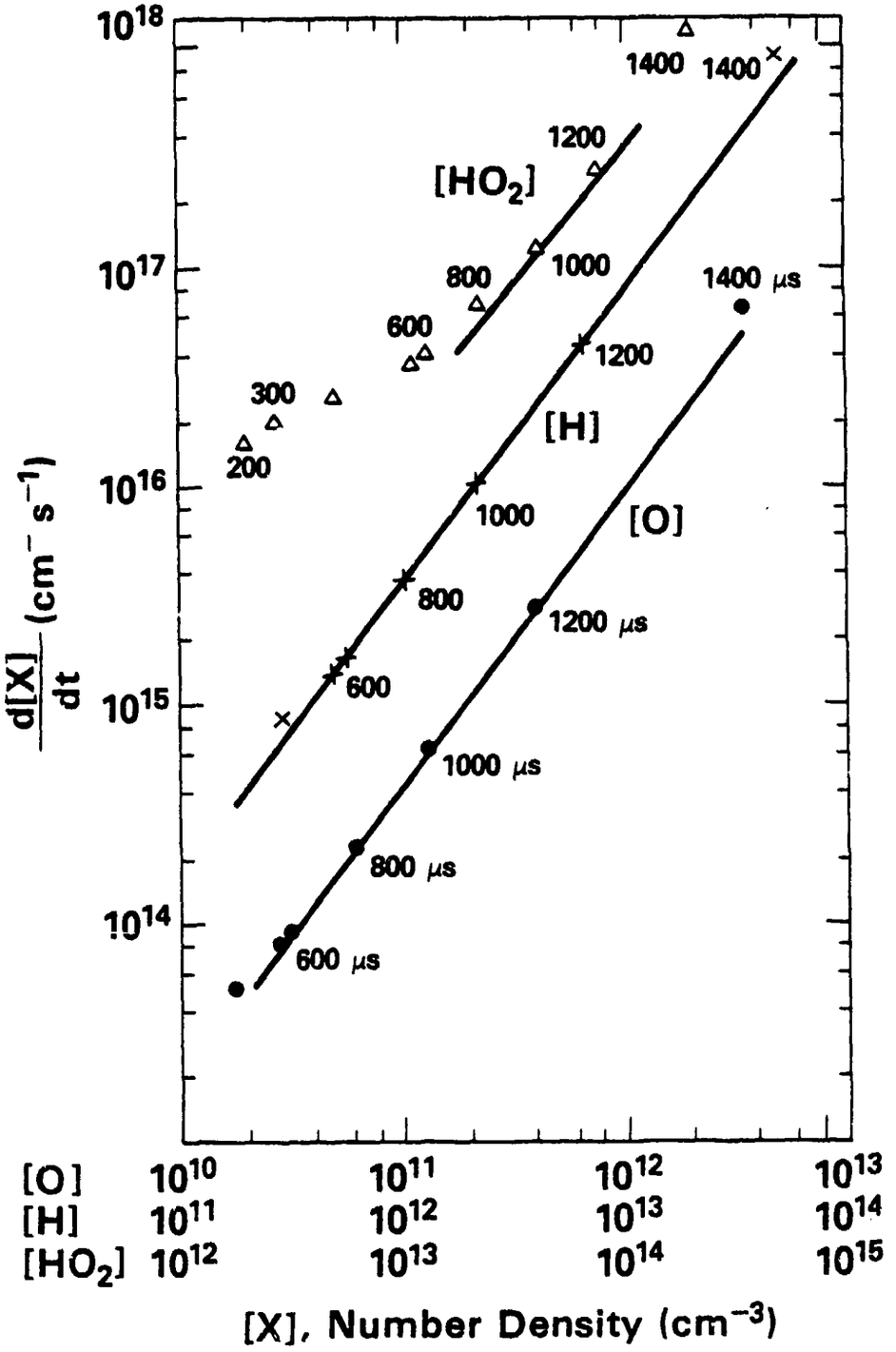


Fig. 12 — Calculated time-rate-of-change of O, H, and $HO_2$ as a function of their density for the weak ignition case

where we have let n = [OH]. The first two terms represent the initial behavior, the $S_1$ term represents an exponential term, and the $S_{4/3}$ term represents the explosive runaway behavior shown in Figures 11 and 12. We consider now only the weak ignition case and first look at an equation of the form

$$\frac{dn}{dt} = S_o + S_{4/3}n^{4/3} \tag{9}$$

By choosing two points, $t_a$ and $t_b$, on the slope 4/3 line on Figure 13b and ensuring that Equation 9 goes through them, we find $S_{4/3}$. Then the data can be used to determine $S_{-1}$ and $S_1$ in the regime below the 4/3 slope according to

$$\frac{dn}{dt} = \frac{S_{-1}}{n} + S_1 n \tag{10}$$

which has the solution

$$n^2(t) = [n^2(0) + \frac{S_{-1}}{S_1}] e^{2S_1 t} - \frac{S_{-1}}{S_1} \quad . \tag{11}$$

We then match this equation to the point $t_a$ and pick values of n(0), $S_{-1}$, and $S_1$ which best reproduce the data. The ratio $S_{-1}/S_1$ may be found by noting that

$$\frac{S_{-1}}{S_1} = n_a^2 \left(\frac{1}{f} - 1\right) \tag{12}$$

where f can be found by iterating the equation

$$1 = [1-f(1-\varepsilon_o)]e^{\psi f} \tag{13}$$

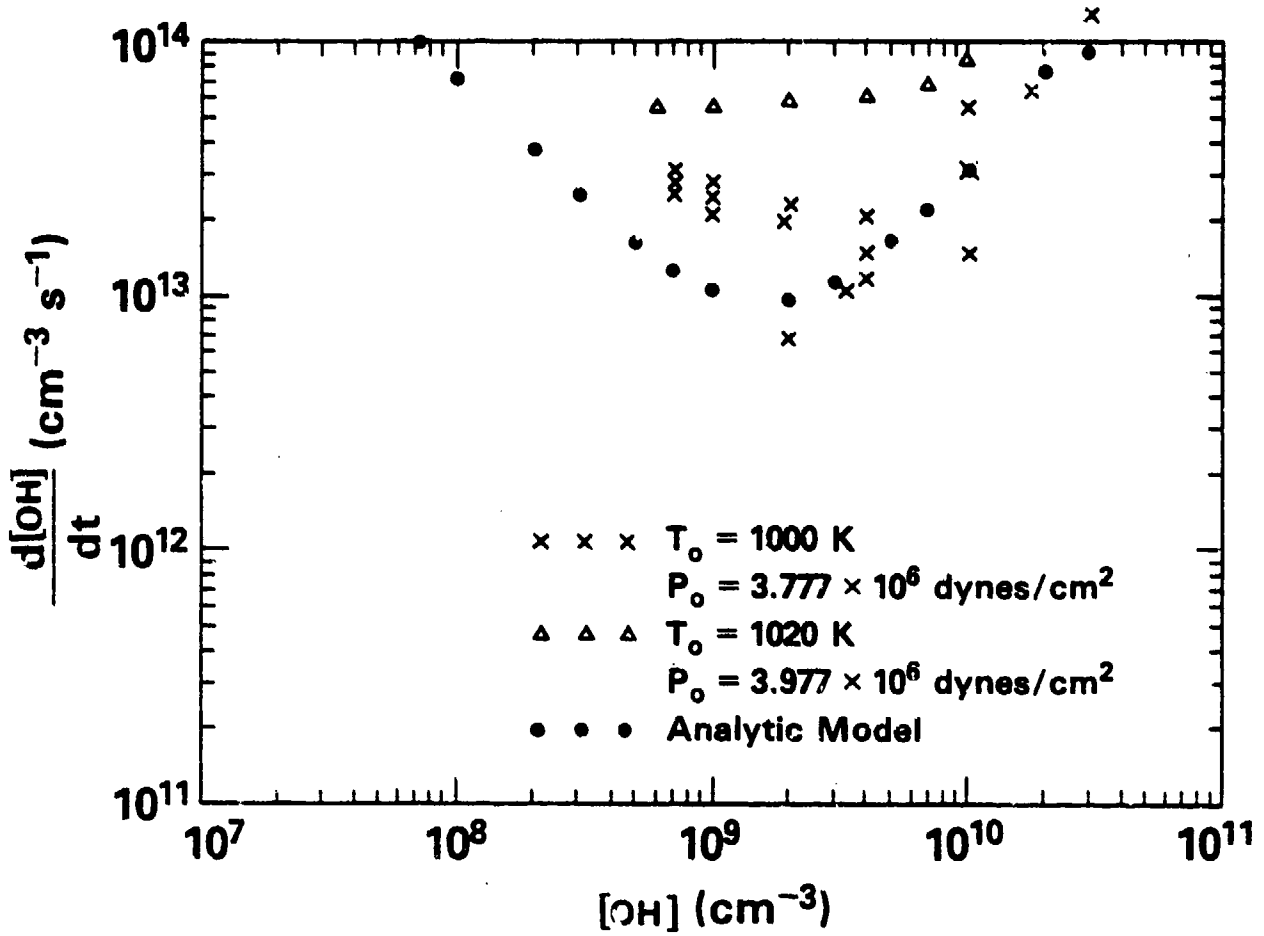


Fig. 13a — Early time behavior of the time-rate-of-change of OH as a function of OH for two sets of pressures and temperatures which correspond to constant entropy. Also shown is the analytic fit.

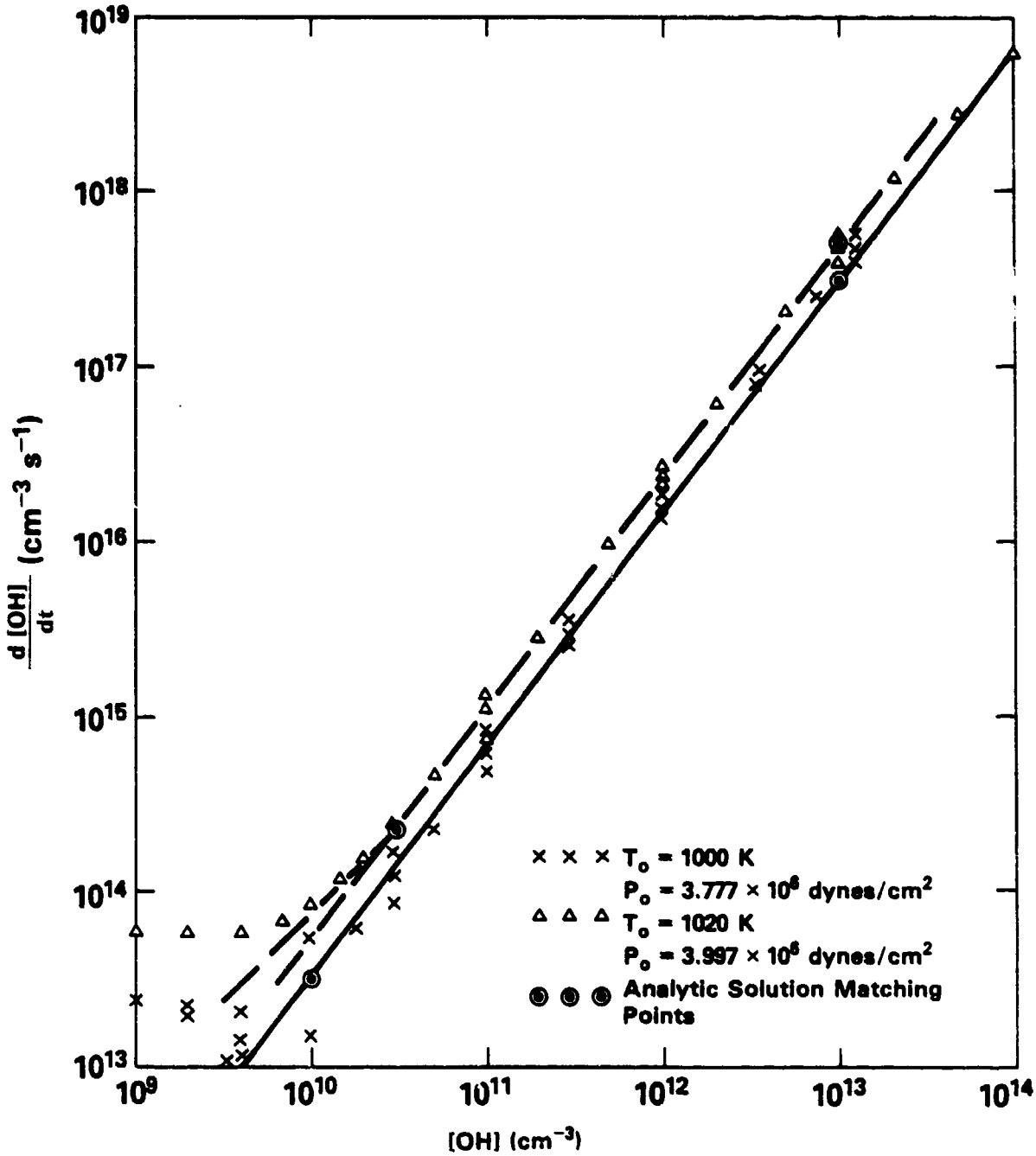


Fig. 13b — Same as Fig. 13a except for later times

with

$$\varepsilon_o = n_o^2/n_a^2 \tag{14}$$

and

$$\psi = \frac{2t_a}{n_a}\frac{dn_a}{dt} \quad . \tag{15}$$

Typical values of the parameters required to solve Equations (9) and (10) for the weak ignition case are given in Table II.

Equation (8) is an ordinary differential equation and thus represents only local variations. Integrating this equation reproduces the detailed chemical behavior shown in Figures 13. To use this simplification we consider an equally spaced set of points which may be described by these equations. We then vary the coefficients at each location as given by the isentropic perturbation resulting from the velocity given in Equation (4). Each point then reaches values of OH signifying ignition at a different time. We use these time differences to evaluate $\Delta\tau_{max}$. Thus we have a simplified, inexpensive way to evaluate a $\Delta\tau_{max}$ which contains the varying chemical sensitivities and is unaffected by communication effects. We have, in effect, a generalized induction parameter model derived from the detailed numerical simulations.

## VI. Prediction of Spotty Ignition

Figure 14 shows $\Delta\tau_{max}$ as a function of $S_L$ for the weak ignition case in Table I for amplitudes of $5x10^2$, $1x10^3$, and $2x10^3$ cm/s. These calculations show that there is a maximum value of $\Delta\tau_{max}$ occuring at a wavelength of $2S_L \approx$ 2-5m. At very short perturbation wavelengths the frequency of oscillation is much faster than the induction time, so phase information

Table II

| $T_o$ | 1000 K | 1020 K |
|---|---|---|
| $P_o$ | $3.777 \times 10^6$ dynes/cm$^2$ | $3.977 \times 10^6$ dynes/cm$^2$ |
| $S_{4/3}$ | 1.4100 | 2.5048 |
| $S_1$ | $2.9659 \times 10^3$ | $7.6872 \times 10^3$ |
| $S_{-1}$ | $7.1843 \times 10^{21}$ | $8.6158 \times 10^{22}$ |

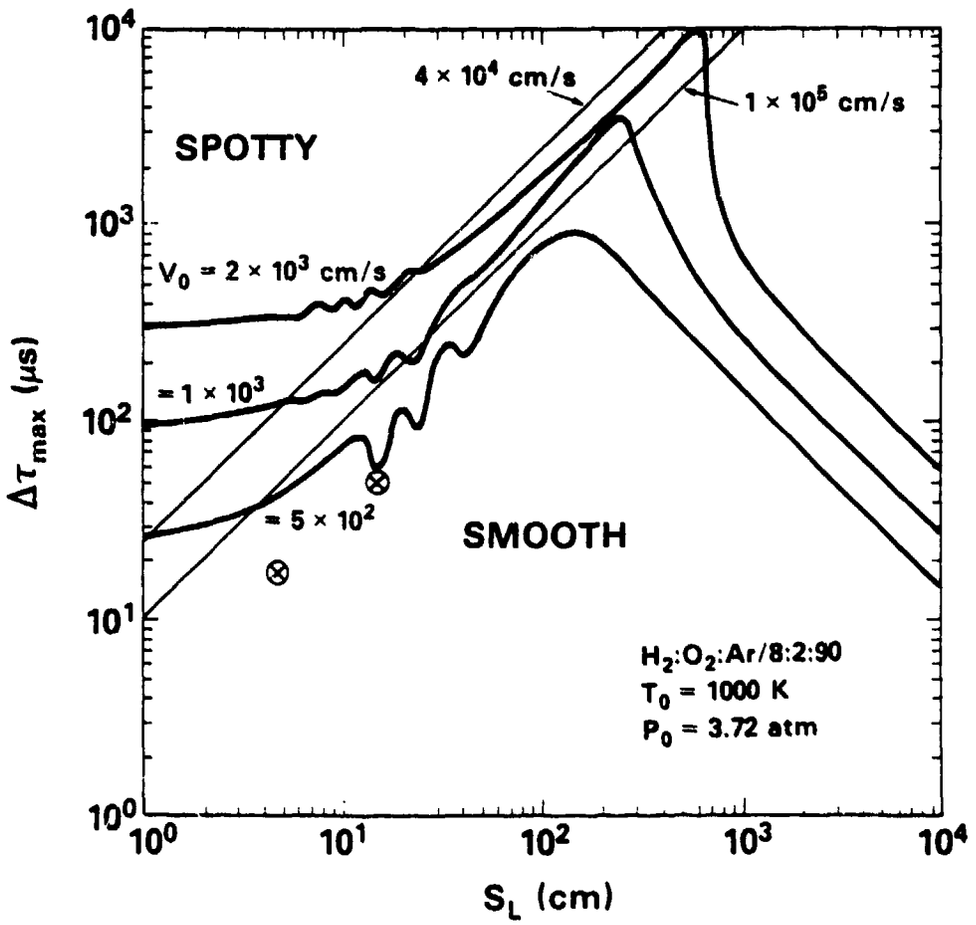


Fig. 14 — Graph of $\Delta\tau_{max}$ as a function of $S_L$ for three sound wave perturbations on the mixture $H_2$:$O_2$:Ar/8:2:90 at 1000 K and 3.72 atm. Also shown are the reflected shock velocity which together with the $\Delta\tau$ separates regimes spotty and smooth ignition.

about the sound wave in various regions of the system averages out. The remaining RMS quadratic effects cause the left and right ends of the system to react slightly faster than the center where the node of the sound wave keeps temperature and pressure constant. This enhanced reactivity is a function of the perturbation amplitude, but not the frequency. Thus the $\Delta\tau_{max}$ $(S_L, v_o)$ curves go to a constant value at the left. The slope of -1, on the right for $\Delta\tau_{max}$ $(S_L, v_o)$ arises in an equally straightforward way. When the wavelength and periods are very long, much longer than the induction time, the temperature and pressure perturbations across the system are very small and vary inversely as the fluctuation period. In this case the induction time difference scales linearly with $\Delta\tau_{max}$, and $\Delta\tau_{max}$ then scales in this limit as $1/S_L$. These mathematical results are upheld by the detailed calculations which also show a weak resonance of the value of $\Delta\tau_{max}$ whenever the induction time is an integral or half integral multiple of the oscillation frequency.

The straight lines on Figure 14 correspond to reflected shock velocities. This theory predicts spotty ignition when a particular $\Delta\tau_{max}$ wavelength-amplitude combination falls to the left of the shock velocity line, and smooth ignition if it falls to the right. Consider for example the case of $S_L$ = 15 cm. When $v_o = 1\times10^3$ cm/s, ignition may be spotty for shock velocities less than about $6\times10^4$ cm/s. As we can see qualitatively from Figure 10 and quantitatively from Figure 25, a higher shock velocity ensures smooth ignition. For the lower amplitude, $5\times10^2$ cm/s, ignition is smooth to a velocity of about $2\times10^5$ cm/sec. We note that the communication effect which tends to lower $\Delta\tau_{max}$ would have

the same qualitative effect as decreasing the amplitude of the perturbation.

Even though the curve for the strong ignition case is not shown in Figure 14 we may still use it to see why spottiness does not occur. Since the induction time was shorter than in a weak ignition case, the value of $S_L$ corresponding to the same number of oscillations in an induction time is much smaller, i.e., 1.13 cm compared to 15 cm. The value of $\Delta\tau_{max}$ $(S_L, v_o)$ is also much smaller for equivalent amplitudes of the perturbation, about 1 μs for $v_o = 5\times10^2$ cm/s. To get spotty ignition the reflected shock velocity would have to be very high. Thus we see two reasons why spottiness would not be detected: 1) we would require very high reflected shock velocities for spottiness to occur and 2) we would have to have 1 μs resolution in the schlieren photography to see spottiness.

In both the strong and weak ignition cases studied in Paper I and summarized in Table I, the velocity perturbations were approximately the same size. Maximum velocities of about $6\times10^3$ cm/s near the reflecting wall decayed quickly to $\sim10^2$-$10^3$ cm/s or less. Reflected shock velocities were 4-$5\times10^4$ cm/s. Thus the strong ignition case falls far into the smooth ignition region and the weak ignition case falls in the spotty ignition region.

## VII. Conclusion

Figures 3 and 4 suggest that certain regions in the pressure-temperature plane are very sensitive to entropy and sound wave perturbations. For a fixed stoichiometry, the more sensitive regions tend to have longer induction times.

The reason for this sensitivity lies in the chemical reactions and rates controlling the radical formation even before any significant amount of energy is released. When the reaction $H + O_2 + M \rightarrow HO_2 + M$ becomes significant compared to $H + O_2 \rightarrow OH + O$, the growth of the radicals becomes faster than exponential. We have seen this in Figures 11-13 in which the slope of log [d[OH]/dt] versus log [OH] changes from 1 to 4/3 at low enough temperatures. We see, for example, that a perturbation on a constant adiabat when the slope is 4/3 would create more of a change in induction time than an adiabatic perturbation on the slope 1 curve.

For a system initially at a given pressure and temperature, we can quantify the sensitivity to a specific form of perturbation by calculating the range of induction times it produces, $\Delta\tau_{max}$ $(S_L, v_o)$. This can always be done using a detailed simulation. However, for the specific case of sound waves, a generalized induction parameter model was derived above based on a parameterization of the calculated behavior of the radical OH.

As shown qualitatively in Figure 10, ignition may be spotty or smooth depending on the relationship of $\Delta\tau_{max}$ to the velocity of the reflected shock and the wavelength of the fluctuation. This result is shown quantitatively in Figure 14 for the weak ignition case. Although the arguments made above were made for sound waves, they also hold in general for entropy perturbations. That is, it is the relation of the $\Delta\tau_{max}$ characteristic of the

perturbation in the system to the velocity of the reflected shock that determines if ignition is spotty. In some cases the $\Delta\tau_{max}$ might be decreased by the communication effect discussed above once energy begins to be released.

Weak and strong ignition can thus be analyzed in terms of what we have learned above. Ignition is weak if the parameters characterizing the system fall onto the spotty side of a picture analogous to Figure 14 and if $\Delta\tau_{max}$ is large enough to be observable. If $\Delta\tau_{max}$ or $S_L$ is too small, ignition will appear smooth. If the sytem falls onto the smooth side of Figure 14, or $\Delta\tau_{max}$ is too small to be observable, ignition appears to be strong. Thus the cut-off between weak and strong ignition depends equally on the sensitivity of the chemical induction time and on the characteristics of the shock tube which allow a certain range of amplitudes and frequencies of sound waves and entropy perturbations to be both generated and measured.

The different criteria proposed by Voevodsky and Soloukhin [8] and Meyer and Oppenheim [9] may be interpreted in these terms. Voevodsky and Soloukhin's determination of the dividing line in the pressure-temperature plane is the extended second limit calculated with particular values of $k_2$ and $k_3$. This is a purely chemical criterion which is independent of the specific form of the driving fluctuation. Meyer and Oppenheim determined experimentally that the dividing line was at $\partial\tau_i/\partial T\Big|_P = -2\mu s K^{-1}$, which occurs for higher temperatures at low pressures. Their criterion depends not only on chemistry but also on a particular type of fluctuation - in this case thermal fluctuations but not sound waves. We conclude that the differences between the two criteria proposed can be explained by different levels of sound and entropy fluctuations in the two experimental systems.

We conclude then that the analysis presented in this paper could be used to provide information about the nonuniformities existing behind shock waves. The possibility also arises of using controlled perturbations to study and calibrate the sensitivity of reactive systems and of using the explosive behavior of the $n^{4/3}$ regime as an amplifier in order to measure very low radical concentrations.


## Acknowledgements

The authors would like to thank Dr. Roger Strehlow for his encouragement and Dr. Theodore Young for his help. This work was sponsored by the Office of Naval Research and the Naval Material Command.


## References


1. Oran, E.S., Young, T.R., Boris, J.P., Cohen, A., Weak and Strong Ignition: I. Numerical Simulations of Shock Tube Experiments, submitted to Combustion and Flame.
2. Cohen, A., and Larsen, J., Explosive Mechanism of the $H_2$-$O_2$ Reaction Near the Second Ignition Limit, B.R.L. Report No. 1386, Ballistics Research Laboratories, Aberdeen, Maryland 1967.
3. Strehlow, R.A., and Cohen, A., Phys. Fluids 5, 97 (1962).
4. Strehlow, R.A., and Dyner, H.B., AIAA Journal 1, 591 (1963).
5. Gilbert, R.B., and Strehlow, R.A., AIAA Journal 4, 1777 (1966).
6. Soloukhin, R.I., Shock Waves and Detonations in Gases, Moscow, FM: 1963; also Doklady Akad. Nauk. SSSR 122, 1039 (1958).
7. Zaitsev, S.G., and Soloukhin, R.I., Eighth Symposium (International) on Combustion, The Williams and Wilkens Co., Baltimore, 1962, p. 335.

8. Voevodsky, V.V., and Soloukhin, R.I., Tenth Symposium (International) on Combustion, The Combustion Institute, Pittsburgh, PA, 1965, p. 279.

9. Meyer, J.W., and Oppenheim, A.K., Thirteenth Symposium (International) on Combustion, The Combustion Institute, Pittsburgh, PA, 1970, p.1153.

10. Borisov, A.A., Acta Astronautica, 1, 909 (1974).

11. Toong, T.-Y., Combustion and Flame 18, 207 (1972).

12. Toong, T.-Y., Acta Astronautica 1, 317 (1974).

13. Garris, C.A., Toong, T.-Y., Patureau, J.-P., Cata Astronautica 2, 981 (1975).

14. T.-Y., Arbeau, P., Garris, C.A., and Patureau, J.-P., Fifteenth Symposium (International) on Combustion, 87 (1974).

15. Patureau, J.-P., Toong, T.-Y., and Garris, C.A., Sixteenth Symposium (International) on Combustion, 927 (1977).

16. Oran, E.S., Boris, J.P., Young, T.R., Flanigan, M., Burks, T., and Picone, M., Eighteenth Symposium (International) on Combustion, p. 1641, The Combustion Institute, Pittsburgh, PA, 1981.

17. Burks, T.L., and Oran, E.S., A Computational Study of the Chemical Kinetics of Hydrogen Combustion, NRL Memorandum Report 4446, Naval Research Laboratory, Washington, D.C., 1980.

18. Oran, E.S., Young, T.R., and Boris, J.P., Seventeenth Symposium (International) on Combustion, The Combustion Institute, 1978, p. 43.

19. Boris, J.P., and Book, D.L., Methods in Computational Physics, Vol. 16, p. 85, Academic Press, 1976.

20. Boris, J.P., Flux-Corrected Transport Modules for Solving Generalized Continuity Equations, Naval Research Laboratory, NRL Memo Report 3237, 1976.

21. Young, T.R., and Boris, J.P., J. Phys. Chem. 81, 2424, (1977).

22. Young, T.R., CHEMEQ, A Subroutine for Solving Stiff Ordinary Differential Equations, NRL Memorandum Report 4091, Naval Research Laboratory, Washington, D.C., 1980.

23. Oran, E.S., and Boris, J.P., Prog. Energy Combustion Science, 7:1 (1981).

24. Schott, G.L., and Getzinger, R.W., Physical Chemistry of Fast Reactions, 1, 81, (1973).

25. Brokaw, R.S., Tenth Symposium (International) on Combustion, p. 269, The Combustion Institute, Pittsburgh, PA, 1965.